Available online at www.sciencedirect.com

SciVerse ScienceDirect

Ceramics International 39 (2013) 3441–3445

CERAMICS INTERNATIONAL

www.elsevier.com/locate/ceramint

Short communication

Bulk (Ti,Cr)N consolidated by pulsed current activated sintering and its mechanical properties

In-Jin Shon[a], Chang-Yul Suh[b], Sujeong Lee[b], Ki-Min Roh[b], Hanjung Kwon[b], Sung-Wook Cho[b], Wonbaek Kim[b,*]

[a]*Division of Advanced Materials Engineering, Research Center of Advanced Materials Development, Chonbuk National University, Jeonbuk 561-756, Republic of Korea*

[b]*Minerals and Materials Processing Division, Korea Institute of Geoscience, Mining and Materials Resources, Daejeon, Republic of Korea*

Received 10 August 2012; received in revised form 28 September 2012; accepted 28 September 2012
Available online 11 October 2012

Abstract

Previously, we synthesized (Ti,Cr)N nanoparticles by the electrical explosion of Cr-plated Ti wires and subsequent gas nitriding. In this study, we report the consolidation of bulk (Ti,Cr)N using pulsed current activated sintering (PCAS). A near-full density (Ti,Cr)N compact was obtained in 7 min at 1600 °C. The microhardness and fracture toughness of (Ti,Cr)N were measured and compared to TiN. The average composition of the sintered (Ti,Cr)N was about $Ti_{0.8}Cr_{0.2}N$. The hardness of the (Ti,Cr)N compact was comparable to monolithic TiN even though its grain size was about 3 times larger and it formed a solid solution with softer CrN. It showed almost a complete intergranular fracture mode with a low toughness value possibly due to the embrittled grain boundaries resulting from slight compositional or density variations.

Keywords: TiN; (Ti,Cr)N; Wire explosion; PCAS

1. Introduction

(Ti,Cr)N is one of the most studied ternary nitride materials to improve the mechanical, optical and physical properties of TiN [1–5]. (Ti,Cr)N films have been reported to exhibit many attractive properties such as high hardness, excellent abrasive wear, oxidation and corrosion resistances [6,7]. Nevertheless, little attention has been paid to the fabrication of bulk (Ti,Cr)N ceramics, probably because of the complexity in the preparation of (Ti,Cr)N particulates and in the subsequent densification without a binder. Recently, Jin et al. [8] reported the synthesis of (Ti,Cr)N nanoparticles by high-temperature nitridation of Cr_2O_3 and TiO_2 nanocomposite powder which was produced by a homogeneous precipitation method with $Cr(NO_3)_3$ and $Ti(OBu)_4$.

The pulsed current activated sintering (PCAS) method has emerged as an attractive technique for sintering high-temperature materials in relatively short time [9,10]. PCAS is similar to conventional hot-pressing, except that the sample is heated by a pulsed electric current that flows through the sample and a die. This process increases the heating rate (up to 1000 °C/min) to a much higher degree than in traditional hot-press sintering.

Electrical wire explosion (EWE) has been suggested as one plausible method to produce various alloys and intermetallic nanoparticles [11–13]. Recently, we synthesized TiN and (Ti,Cr)N nanoparticles by EWE [14,15]. In this study, (Ti,Cr)N nanopowders were consolidated into a bulk (Ti,Cr)N compact using PCAS and its microhardness and fracture toughness were evaluated.

2. Experimental Procedures

The Ti–Cr wire used for the electrical wire explosion was prepared by electrodeposition of Cr on a 0.289 mm diameter Ti wire. The final diameter of the Cr-coated Ti wire was 0.320 mm which should give an average composition of

*Corresponding author. Tel.: +82 42 868 3623; fax: +82 42 868 3415.
E-mail address: wbkim@kigam.re.kr (W. Kim).

0272-8842/$ - see front matter © 2012 Elsevier Ltd and Techna Group S.r.l. All rights reserved.
http://dx.doi.org/10.1016/j.ceramint.2012.09.097

about 25 at% Cr. The explosion of the Ti–Cr wire in Ar produced a mixture of α-Ti, $TiCr_2$, and Ti-rich β phases [11]. After the explosion, the powders were heated in a tube furnace to synthesize (Ti,Cr)N at 1100 °C with a heating rate of 10 °C/min under flowing nitrogen gas [15].

The (Ti,Cr)N nanopowders were then charged into a graphite die (outside diameter of 45 mm, inside diameter of 10 mm, and height of 40 mm) and placed in the PCAS system (Eltek, South Korea). The sintering was conducted typically in four stages. The system was evacuated (stage 1) and subjected to an uniaxial pressure of 80 MPa (stage 2). An induced current was activated and maintained until densification occurred as indicated by a linear gauge measuring sample shrinkage (stage 3). The temperature was measured by an optical pyrometer that was focused on the surface of the graphite die. The sintering continued until the shrinkage reached a constant value. Afterwards, the compact was cooled to room temperature (stage 4).

The sintered (Ti,Cr)N compact was polished with diamond paste and etched using H_2O (10 mL), glacial acetic acid (10 mL), and HNO_3 (10 mL) for metallographic observation. The phases and composition were analyzed by X-ray diffraction (XRD) and scanning electron microscopy (SEM) with energy dispersive X-ray analysis (EDAX).

The Vickers hardness was measured on the polished surface of the compact using a 1 kg_f load and a 15-s dwell time. The reported values represent an average of five measurements. Indentations produced with sufficiently large loads were characterized by median cracks around the indent. From the lengths of these cracks, one can estimate the fracture toughness of the material using the following expression [16]:

$$K_{IC} = 0.203(c/a)^{-3/2} H_v a^{1/2}$$

where c is the trace length of the crack measured from the center of the indentation, a is half the average length of the two indent diagonals, and H_v is the Vickers hardness.

3. Results and discussion

3.1. Physical properties of (Ti,Cr)N

The formation of (Ti,Cr)N nanoparticles was confirmed by X-ray diffraction and FE-TEM. Fig. 1 shows a FE-TEM image of the (Ti,Cr)N nanoparticles. The EDS and diffractogram obtained from a particle (marked by a circle) suggests that it is a solid solution of TiN and CrN. Fig. 2(a) shows the X-ray diffraction pattern of (Ti,Cr)N nanoparticles where the positions of TiN (JCPDS 38-1420) and CrN (JCPDS 11-0065) are marked by —— and ————, respectively. The angles of the peaks reside between those of TiN and CrN again suggesting the formation of a (Ti,Cr)N solid solution. The lattice parameter of the (Ti,Cr)N nanopowders was calculated to be 0.41957 nm.

The crystal structure of the (Ti,Cr)N nanopowders was retained during the PCAS process. Fig. 2(b) shows the X-ray diffraction pattern of the sintered compact. The peak

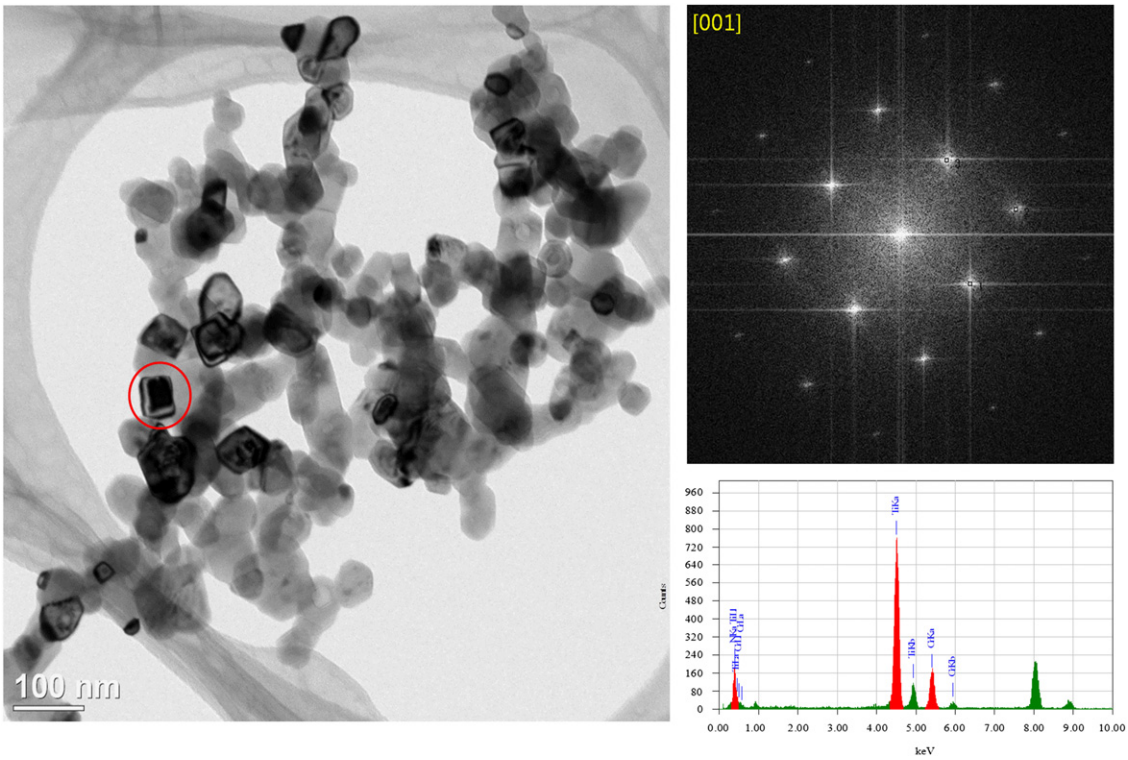

Fig. 1. FE-TEM image, diffractogram, and EDS spectrum of a (Ti,Cr)N nanoparticle which was prepared by EWE and subsequent gas nitriding at 1100 °C for 1 h.

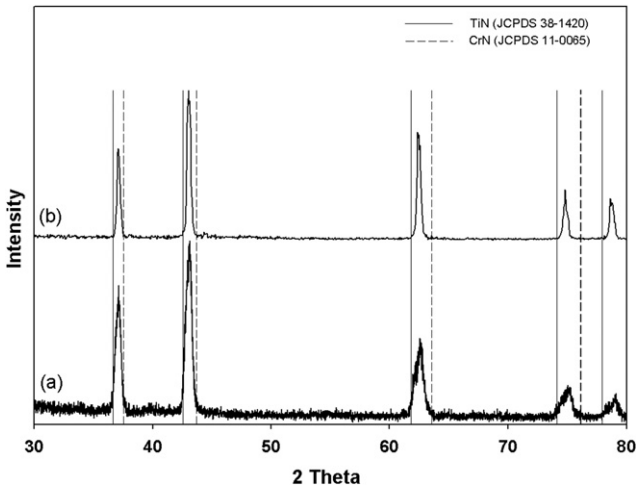

Fig. 2. X-ray diffraction patterns of (Ti,Cr)N: (a) nanopowders prepared by EWE of Cr-plated Ti wire and subsequent gas nitriding at 1100 °C for 1 h and (b) bulk sintered at 1600 °C.

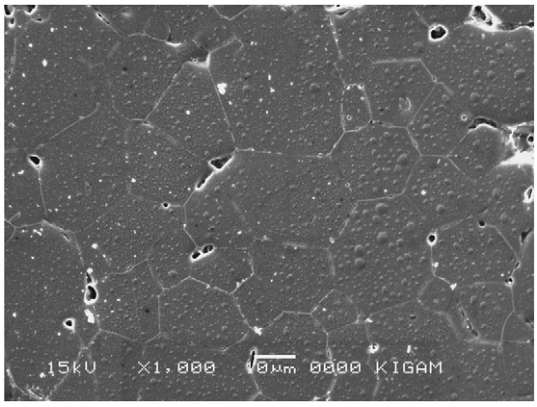

Fig. 3. SEM micrograph of the polished and etched surface of the sintered (Ti,Cr)N compact at 1600 °C.

became much sharper indicating considerable grain coarsening. The average grain size measured metallographically was about 19.8 μm which is significantly larger than that of TiN (7.1 μm) [17]. Fig. 3 shows the polished and etched surface of the (Ti,Cr)N compact. The lattice parameter of the sintered (Ti,Cr)N was 0.42038 nm. Examination of the sintering–shrinkage curve explains the coarse grain size of the (Ti,Cr)N compact. In the case of TiN, the consolidation was accomplished in 2 min while (Ti,Cr)N required almost 7 min (Fig. 4). This suggests that the consolidation of (Ti,Cr)N was much more tedious than with TiN. This result is quite reasonable considering that mutual diffusion of Ti and Cr should occur unlike with monolithic TiN.

As previous stated, information on the bulk form of (Ti,Cr)N is not available except for the report by Jin et al. [8]. They synthesized a series of $Cr_{1-x}Ti_xN$ powders by the high temperature nitriding of Cr_2O_3 and TiO_2 nanocomposite powders. They found that the lattice parameter of CrN increased linearly with the amount of TiN. Fig. 5 displays their data along with the results obtained in our study. The extrapolation of their data for pure TiN ($x=1$)

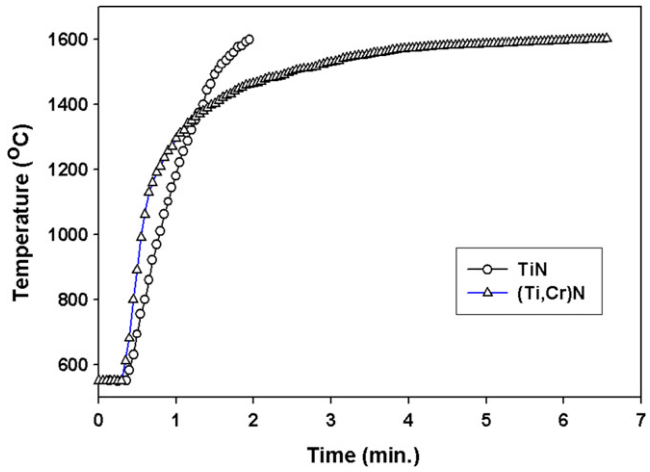

Fig. 4. Sintering temperature history of (Ti,Cr)N and TiN during the PCAS process.

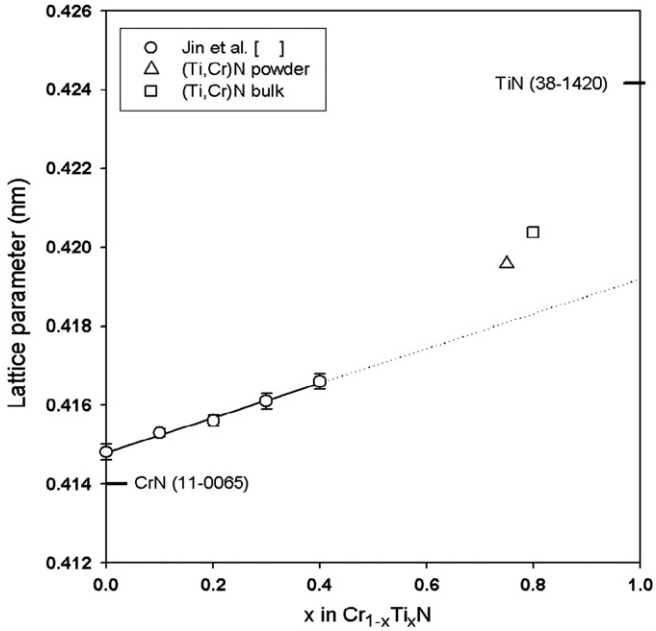

Fig. 5. The effect of the TiN solution on the lattice parameter of $Cr_{1-x}Ti_xN$.

shows a significantly lower value than the reference (TiN JCPDS 38-1420). The value is even lower than the results for (Ti,Cr)N obatined in this study for a solid solution with CrN. This large discrepancy appears to originate from the synthesis method. Obviously, more study is necessary to better understand the physical properties of (Ti,Cr)N.

3.2. Mechanical properties of bulk (Ti,Cr)N

The Vickers hardness and fracture toughness of (Ti,Cr)N were measured and are tabulated in Table 1 with our previously obtained data for monolithic TiN [17]. The grain size of (Ti,Cr)N is about 3 times larger than that of TiN. The hardness of the (Ti,Cr)N compact (1712 kg/mm^2)

Table 1
Summary of the mechanical properties of bulk (Ti,Cr)N and TiN consolidated by pulsed current activated sintering at 1600 °C.

	(Ti,Cr)N	TiN [17]
Vickers hardness (kg/mm^2)	1712	1650
Fracture toughness (MPa m$^{1/2}$)	3.5	6.0
Average grain size (μm)	19.8	7.1

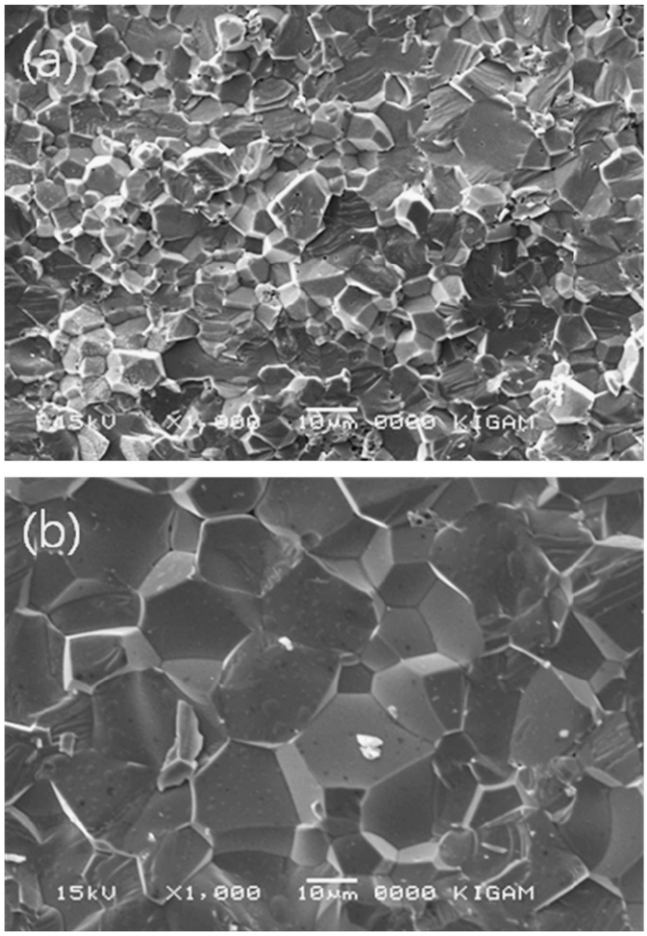

Fig. 6. SEM micrographs of the fracture surfaces of sintered compacts at 1600 °C using PCAS: (a) TiN and (b) (Ti,Cr)N.

was slightly higher or comparable to that of pure TiN (1650 kg/mm^2). This result was not expected based on two considerations as follows. Jin et al. [8] reported that the microhardness of $Cr_{1-x}Ti_xN$, the solid solution of TiN and CrN, increased linearly with x as follows:

$$H = 14.895 + 8.625x \text{ (GPa)}$$

Accordingly, TiN should have the maximum hardness in the $Cr_{1-x}Ti_xN$ series. Moreover, a Hall–Patch type relationship between the grain size and hardness has been known to exist in ceramic materials [18,19]. Therefore, the hardness of (Ti,Cr)N would be reduced by both the formation of a solid solution with the softer CrN and by the larger grain size. Obviously, the reason for this discrepancy is not clear. It may be that there is a solution hardening mechanism working for (Ti,Cr)N, as suggested by other researchers even though it was for thin films [8,20].

The interpretation on the effect of the grain size on the fracture toughness appears to be much more diverse than the effect on the hardness. In previous works, the fracture toughness showed a maximum with grain size [21–24], decreased with grain size [25,26], increased with grain size [27–29], or showed no grain-size dependence [30,31].

In this study, the fracture toughness of the coarser-grained (Ti,Cr)N was significantly lower than that of monolithic TiN (Table 1). Fig. 6(a) and (b) shows the fracture surfaces of the TiN and (Ti,Cr)N compacts. Both reveal a mixture of intergranular and transgranular fracture modes. Nevertheless, the degree of intergranular fracture appears to be more pronounced in the (Ti,Cr)N. This is not common considering that fine-grained ceramics usually favor intergranular fracture and large-grained ceramics experience transgranular fracture [25]. The dominant intergranular fracture of the coarse-grained (Ti,Cr)N suggests that the grain boundaries of (Ti,Cr)N may be embrittled favoring the intergranular fracture. The reason could be the slight compositional or density variations in the grain boundaries of (Ti,Cr)N. It is possible that the difference of the fracture toughnesses of TiN and (Ti,Cr)N arises from the grain or grain-boundary chemistry rather than the grain size alone. In any case, it is obvious that a more controlled study is needed for better understanding of the lower toughness of bulk (Ti,Cr)N.

4. Conclusions

In this study, we report the consolidation of single-phase (Ti,Cr)N nanoparticles into bulk (Ti,Cr)N using pulsed current activated sintering (PCAS). A near-full density (Ti,Cr)N compact was obtained in 7 min at 1600 °C. The hardness of (Ti,Cr)N compact was slightly higher than that of TiN. The fracture toughness of (Ti,Cr)N was significantly lower than TiN showing a predominantly intergranular fracture. The hardness and fracture toughness of bulk (Ti,Cr)N were 1712 kg/mm^2 and 3.5 MPa m$^{1/2}$, respectively.

Acknowledgments

This study was supported by a grant from the Basic Research Project of Korea Institute of Geoscience.

References

[1] H.A. Jehn, F. Thiergarten, E. Ebersbach, D. Fabian, Characterization of PVD (Ti,Cr)N_x hard coatings, Surface and Coatings Technology 50 (1991) 45–52.
[2] Y. Massiani, P. Gravier, L. Fedrizzi, F. Marchetti, Corrosion behavior in acid solution of (Ti,Cr)N_x films deposited on glass, Thin Solid Films 261 (1995) 202–208.
[3] Y. Otani, S. Hofmann, High temperature oxidation behavior of ($Ti_{1-x}Cr_x$)N coatings, Thin Solid Films 287 (1996) 188–192.

[4] J.J. Nainaparampil, J.S. Zabinski, A. Korenyi-Both, Formation and characterization of multiphase film properties of (Ti–Cr)N formed by cathodic arc deposition, Thin Solid Films 333 (1998) 88–94.
[5] K.H. Lee, C.H. Park, Y.S. Yoon, J.J. Lee, Structure and properties of $(Ti_{1-x}Cr_x)N$ coatings produced by the ion-plating method, Thin Solid Films 385 (2001) 167–173.
[6] Y. Otani, S. Hofmann, High temperature oxidation behavior of $(Ti_{1-x}Cr_x)N$ coatings, Thin Solid Films 287 (1996) 188–192.
[7] D.E. Wolfe, B.M. Gabriel, M.W. Reedy, Nanolayer (Ti,Cr)N coatings for hard particle erosion resistance, Surface and Coatings Technology 205 (2011) 4569–4576.
[8] X. Jin, L. Gao, J. Sun, Preparation of nanostructured $Cr_{1-x}Ti_xN$ ceramics by spark plasma sintering and their properties, Acta Materialia 54 (2006) 4035–4041.
[9] I.Y. Ko, J.H. Park, K.S. Nam, I.J. Shon, Rapid consolidation of nanocrystalline $NbSi_2$–Si_3N_4 composites by pulsed current activated combustion synthesis, Metals and Materials International 16 (2010) 393–398.
[10] I.J. Shon, S.L. Du, I.Y. Ko, J.M. Doh, J.K. Yoon, J.H. Park, Effect of Fe_2O_3 on properties and densification of 8YSZ by pulsed current activated sintering, Electronic Materials Letters 7 (2011) 133–137.
[11] W. Kim, J.S. Park, C.Y. Suh, S.W. Cho, S. Lee, Ti–Cr nanoparticles prepared by electrical wire explosion, Materials Transactions 50 (2009) 2344–2346.
[12] W. Kim, J.S. Park, C.Y. Suh, H. Chang, J.C. Lee, Fabrication of alloy nanopowders by the electrical explosion of electrodeposited wires, Materials Letters 61 (2007) 4259–4261.
[13] W. Kim, J.S. Park, C.Y. Suh, J.G. Ahn, J.C. Lee, Cu–Ni–P alloy nanoparticles prepared by electrical wire explosion, Journal of Alloys and Compound 465 (2008) L4–L6.
[14] W. Kim, J.S. Park, C.Y. Suh, S.W. Cho, S. Lee, I.J. Shon, Synthesis of TiN nanoparticles by explosion of Ti wire in nitrogen gas, Materials Transactions 40 (2009) 2897–2899.
[15] S. Lee, W. Kim, C.Y. Suh, S.W. Cho, T. Ryu, J.S. Park, I.J. Shon, Preparation of titanium–chromium nitride by gas nitriding of the explosion products of Cr-coated Ti wire, Materials Transactions 52 (2011) 261–264.
[16] K. Niihara, Indentation microfracture of ceramics—its application and problems, Ceramic Society of Japan 20 (1985) 12–18.
[17] W. Kim, J.S. Park, S.W. Cho, N.R. Kim, I.Y. Ko, I.J. Shon, Properties and rapid consolidation of binderless titanium nitride by pulsed current activated sintering, Journal of Ceramic Processing Research 11 (2010) 627–630.
[18] A. Krell, P. Blank, Grain size dependence of hardness in dense submicrometer alumina, Journal of the American Ceramic Society 78 (1995) 1118–1120.
[19] J. Seidel, N. Claussen, J. Rödel, Reliability of alumina ceramics: effect of grain size, Journal of the European Ceramic Society 15 (1995) 395–404.
[20] X. Zeng, S. Zhang, J. Hsieh, Development of graded Cr–Ti–N coatings, Surface and Coatings Technology 102 (1998) 108–112.
[21] A.F. Bower, M. Ortiz, The influence of grain size on the toughness of monolithic ceramics, Transactions of the American Society for Metals 115 (1993) 228–236.
[22] H. Kodama, T. Miyoshi, Study of fracture behavior of very fine-grained silicon carbide ceramics, Journal of the American Ceramic Society 73 (1990) 3081–3086.
[23] L.D. Monroe, J.R. Smyth, Grain size dependence of fracture energy of Y_2O_3, Journal of the American Ceramic Society 61 (1978) 538–539.
[24] R.W. Rice, Grain size and porosity dependence of ceramic fracture energy and toughness at 22 °C, Journal of Materials Science 31 (1996) 1969–1983.
[25] A. Muchtar, L.C. Lim, Indentation fracture toughness of high purity submicron alumina, Acta Materialia 46 (1998) 1683–1690.
[26] M.V. Swain, Grain-size dependence of toughness and transformability of 2 mol% Y-TZP ceramics, Journal of Materials Science Letters 5 (1986) 1159–1162.
[27] G. Vekinis, M.F. Ashby, P.W.R. Beaumont, R-curve behavior of Al_2O_3 ceramics, Acta Metallurgica et Materialia 38 (1990) 1151–1162.
[28] K.-H. Zum Gahr, W. Bundschuh, B. Zimmerlin, Effect of grain size on friction and sliding wear of oxide ceramics, Wear 162–164 (1993) 269–279.
[29] B. Mussler, M.V. Swain, N. Claussen, Dependence of fracture toughness of alumina on grain size and test technique, Journal of the American Ceramic Society 65 (1982) 566–572.
[30] W. Yao, J. Liu, T.B. Holland, L. Huang, Y. Xiong, J.M. Schoenung, A.K. Mukherjee, Grain size dependence of fracture toughness for fine grained alumina, Scripta Materialia 65 (2011) 143–146.
[31] T. Tani, Y. Miyamoto, M. Koizumi, M. Shimada, Grain size dependence of Vickers microhardness and fracture toughness in Al_2O_3 and Y_2O_3 ceramics, Ceramics International 12 (1986) 33–37.